NANO LETTERS

LETTER

pubs.acs.org/NanoLett

Plasmon Resonant Enhancement of Photocatalytic Water Splitting Under Visible Illumination

Zuwei Liu,[‡] Wenbo Hou,[§] Prathamesh Pavaskar,[†] Mehmet Aykol,[†] and Stephen B. Cronin*[,†,‡,§]

Departments of [†]Electrical Engineering, [‡]Physics, and [§]Chemistry, University of Southern California, Los Angeles, California 90089, United States

Supporting Information

ABSTRACT:

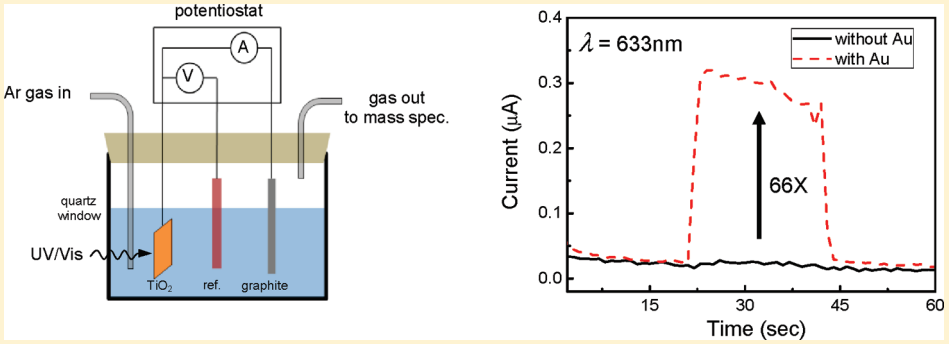

We demonstrate plasmonic enhancement of photocatalytic water splitting under visible illumination by integrating strongly plasmonic Au nanoparticles with strongly catalytic TiO_2. Under visible illumination, we observe enhancements of up to 66× in the photocatalytic splitting of water in TiO_2 with the addition of Au nanoparticles. Above the plasmon resonance, under ultraviolet radiation we observe a 4-fold reduction in the photocatalytic activity. Electromagnetic simulations indicate that the improvement of photocatalytic activity in the visible range is caused by the local electric field enhancement near the TiO_2 surface, rather than by the direct transfer of charge between the two materials. Here, the near-field optical enhancement increases the electron−hole pair generation rate at the surface of the TiO_2, thus increasing the amount of photogenerated charge contributing to catalysis. This mechanism of enhancement is particularly effective because of the relatively short exciton diffusion length (or minority carrier diffusion length), which otherwise limits the photocatalytic performance. Our results suggest that enhancement factors many times larger than this are possible if this mechanism can be optimized.

KEYWORDS: Plasmonic, photocatalytic, photocatalysis, water splitting, anodic titanium oxide, enhancement, FDTD

Solar energy presents a promising alternative as an abundant, largely untapped resource. The amount of energy striking the Earth from sunlight in one hour (4.3×10^{20} J) is more than the total energy consumed on this planet in one year (4.1×10^{20} J). Photocatalysis provides a method for storing the sun's energy in chemical bonds that can be released later without producing harmful byproducts. This has several advantages over direct solar-to-electric conversion. Traditional photocatalysts are able to efficiently convert solar to chemical energy under ultraviolet illumination, but not under visible illumination. Photocatalytic water splitting has been of great interest since the early 1970s after the first demonstration under ultraviolet radiation by Fujishima and Honda.[1] While TiO_2 is one of the most promising photocatalysts, it does not absorb light in the visible region of the electromagnetic spectrum. Because of TiO_2's short wavelength cutoff, there are very few solar photons (~4%) that can be used to drive this photocatalyst. Several attempts have been made previously to extend the cutoff wavelength of this catalyst, including doping[2,3] and defect creation.[4] While these efforts have resulted in slight improvements in the absorption in the visible range, leaving a majority of the solar spectrum unable to drive this photocatalyst,[2,3,5] the approach described in this Letter represents a new mechanism that can be added to and combined with these previous methods for further enhancement.

Plasmon resonant nanostructures have gained considerable interest in many fields, including near-field optics,[6,7] surface enhanced spectroscopy,[8−11] solar cells,[19] and medicine.[14,15] More recently, researchers have explored the applicability of plasmonic processes in the field of photocatalytic chemistry for organic molecule decomposition,[16,17] CO oxidation,[18] and even materials synthesis.[12,13] Various enhancement mechanisms have been proposed, including plasmonic heating and charge transfer.

Received: November 15, 2010
Revised: January 30, 2011
Published: February 14, 2011

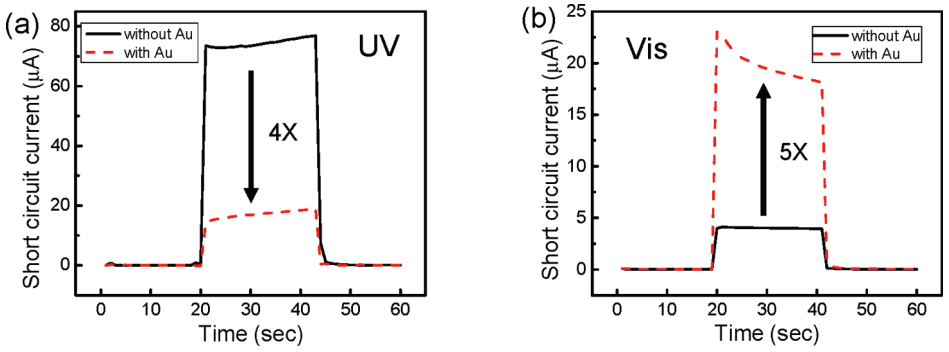

Figure 1. Photocurrent of anodic TiO_2 with and without Au nanoparticles at zero bias voltage irradiated with (a) UV (λ = 254 nm) and (b) visible (λ = 532 nm) light for 22 s.

Tian et al. observed enhanced photocatalytic oxidation of ethanol and methanol in TiO_2 films loaded with gold nanoparticles.[20] Noble-metal-loaded titania photoreactions were also studied by Kowalska et al.[21] These results were attributed to a charge transfer mechanism in which the plasmon-induced charge in the Au nanoparticle transfers an electron to the TiO_2 conduction band, leaving behind a hole that is filled by a donor ion from solution.[22] This depiction of holes and electrons resembles that of a dye-sensitized solar cell, but is not realistic for electrons in a metal.[23,24] This model implies that a surface plasmon is similar in nature to an electron−hole pair. However, there is no highest occupied molecular orbital−lowest unoccupied molecular orbital (HOMO−LUMO) energy separation or analogous valence band-conduction band energy separation in a plasmon excitation. Furthermore, the energy band alignment of anatase TiO_2 with respect to the work function of Au is energetically unfavorable for the direct transfer of electrons from Au to TiO_2. While electron transport at metal−semiconductor interfaces is well-known among the electrical engineering community (i.e., the Schottky diode), no rigorous model for this process has been put forth in the context of plasmonics or catalysis.

Here, we demonstrate enhanced photocatalytic water splitting under visible illumination in TiO_2 films by exploiting the large plasmon resonance of Au nanoparticles. Electromagnetic simulations of the Au nanoparticle/TiO_2 composite provide a quantitative basis for determining the underlying photocatalytic enhancement mechanism. This model is based solely on the near-field optical enhancement of the Au nanoparticles. No direct transfer of charge from the plasmonic metal to the catalytic metal oxide is needed to explain the experimental data. Enhanced light absorption and photocurrents in solar cells have been reported using a similar plasmonic enhancement mechanism.[19] Here, we utilize the plasmonic near-field coupling to improve TiO_2 photocatalysis in the visible wavelength range.

We prepare TiO_2 in the anatase crystalline phase by electrochemically oxidizing titanium foils in an ethylene glycol electrolyte containing 0.25 wt % NH_4F and 2 wt % H_2O at an anodization potential of 30 V for two hours, using a graphite rod as the cathode.[25] A more detailed description of this process is given in the Supporting Information. We then evaporate a gold film with a nominal thickness of 5 nm on the surface of the TiO_2. This thin gold film is known to form islandlike growth that is strongly plasmonic and serves as a good substrate for surface enhanced Raman spectroscopy (SERS).[9,10] Absorption spectra of the bare TiO_2 and Au nanoparticle/TiO_2 films were recorded on a Perkin-Elmer Lambda 950 UV/vis/NIR with an integrating sphere detector. We measured the photocatalytic reaction rates of TiO_2 with and without Au nanoparticles in a 1 M KOH solution using a three-terminal potentiostat with the TiO_2 film, a Ag/AgCl electrode, and a graphite electrode functioning as the working, reference, and counter electrodes, respectively, as shown schematically in the Supporting Information. Photocurrent spectra were measured using a Fianium supercontinuum white light source in conjunction with a Princeton Instruments double grating monochromator, providing continuously tunable monochromatic light (10 nm fwhm) from 400 to 1600 nm.

Figure 1 shows the photocurrent of anodic TiO_2 with and without Au nanoparticles irradiated with ultraviolet (20 mW/cm^2 at 254 nm) and visible light (7 W/cm^2 at 532 nm) for 22 s. Under UV illumination (Figure 1a), the addition of gold nanoparticles results in a 4-fold reduction in the photocurrent. This reduction is due to the presence of the gold nanoparticles, which reduces both the photon flux reaching the TiO_2 surface and the surface area of TiO_2 in direct contact with the aqueous solution. Under visible irradiation (λ = 532 nm) (Figure 1b), however, the addition of gold nanoparticles results in a 5-fold increase in the photocurrent due to the large plasmonic enhancement of the local electromagnetic fields. The transient decay observed in Figure 1b is the result of charge trapped at the TiO_2 surface that is released upon irradiation.[26] The comparisons made here are between photocatalytic data taken at the same intensity for each wavelength (254 and 532 nm). As such, these enhancement factors and reduction factors are independent of the relative intensity of the two light sources. Furthermore, we have demonstrated that the photocurrent increases linearly with light intensity, while the enhancement ratio remains constant.

The photocurrents plotted in Figure 1 correspond to short circuit currents obtained under zero applied bias voltage. Figure 2 shows the complete $I-V$ characteristics of TiO_2 with and without Au nanoparticles taken under continuous UV and visible irradiation. Again, when gold nanoparticles are deposited on the TiO_2, we see a drop in the photocurrent under UV irradiation and an increase under visible illumination, over the whole range of applied bias voltages. The enhancement ratios shown in Figures 1 and 2 are slightly different. Figure 2 represents the behavior of most samples, while Figure 1 is the highest enhancement ratio observed in this work. The random nature of the Au nanoparticle film produces large variations in performance; a limitation that can likely be improved by using a more regular array of plasmonic nanoparticles.

The photocatalytic enhancement observed under 633 nm wavelength illumination (0.15 W/cm^2) is shown in Figure 3.

dx.doi.org/10.1021/nl104005n |*Nano Lett.* 2011, 11, 1111–1116

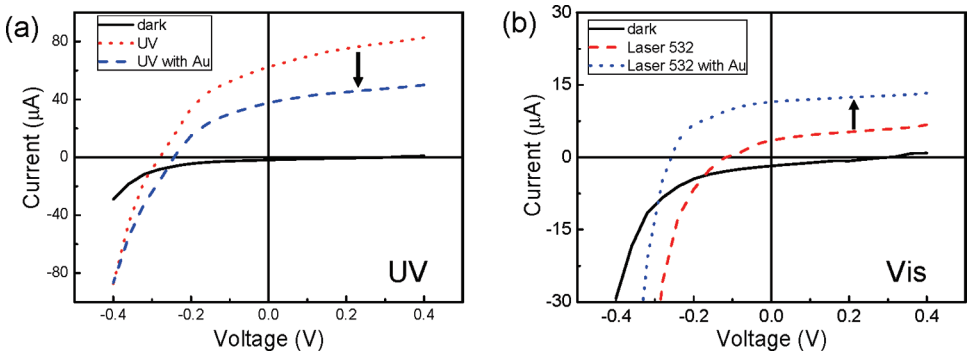

Figure 2. Photocurrent versus bias voltage of anodic TiO_2 with and without Au nanoparticles irradiated with (a) UV and (b) visible light.

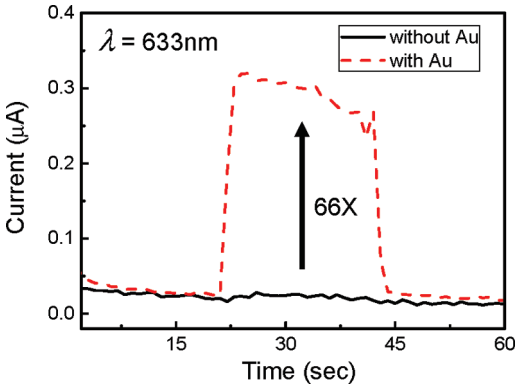

Figure 3. Photocurrent of anodic TiO_2 with and without Au nanoparticles irradiated with λ = 633 nm light for 22 s.

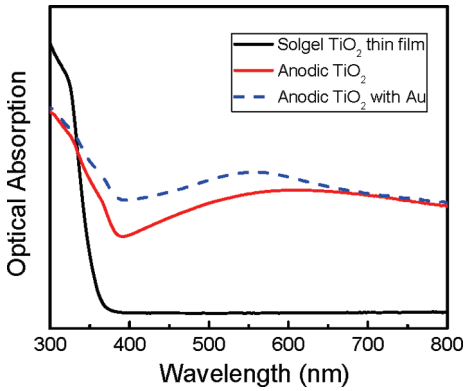

Figure 4. UV−vis absorption spectra of TiO_2 with and without gold nanoparticles.

For bare TiO_2 with no nanoparticles, a small photocurrent of 4.5 nA can be seen just above the noise signal. Here, a significant enhancement in the photocurrent (66×) is evident for the sample with plasmonic Au nanoparticles, resulting in a photocurrent of 0.3 μA. While this irradiation (1.96 eV) is significantly below the bandgap of TiO_2 (3.2 eV), the photocatalytic enhancement is considerably larger than that observed at 532 nm (2.42 eV).

Figure 4 shows the UV−vis absorption spectra of TiO_2 with and without gold nanoparticles. The spectrum taken for an undoped TiO_2 film prepared by the sol−gel method (solid black curve) shows transparency for wavelengths above 370 nm.[27,28] However, the anodic TiO_2 film (red solid curve) shows significant absorption in the visible range, due to N- and F-impurities produced during the anodization process,[29] which create defect states in the bandgap.[30] The absorption spectrum taken from anodic TiO_2 with gold nanoparticles (dashed blue curve) exhibits a slight increase in the absorption in the visible light range. The broad absorption of the Au nanoparticle film is a result of the inhomogeneity in size, shape, and separation of these plasmonic nanoparticles, as can be seen in the electron microscope image of Figure 6a. As a control experiment, we also tested the photocatalytic activity of the undoped TiO_2 prepared by the sol−gel method. No photocurrent was observed for this material with or without Au nanoparticles indicating the importance of defects in the photocatalytic enhancement process under visible illumination.

Figure 5a shows the photocurrent spectra of anodic TiO_2 with and without Au nanoparticles. Both spectra show an appreciable photocurrent for wavelengths below 500 nm. By taking the ratio of these photocurrents (Figure 5b), an enhancement in the photocurrent of TiO_2 with Au nanoparticles can be seen for wavelengths above 500 nm with a maximum enhancement occurring around 650 nm.

Several possible mechanisms may contribute to the enhanced photocurrent observed in the visible wavelength range. First, we can exclude plasmonic heating, since water-splitting requires an energy of 1.32 eV, which is much higher than the thermal energy generated by plasmonic heating.[31] This stands in contrast to organic material decomposition reported by several groups,[16,17] which can be partially attributed to local heating effects.[32,33] Another possible mechanism is enhancement of electron−hole lifetime at the metal/semiconductor interface, which results in increased exciton diffusion lengths. However, considering the small grain size in the anodic TiO_2,[34] the contribution from an increased exciton diffusion length can be ruled out. Several groups have discussed a charge transfer model as a possible explanation for the enhanced photocatalytic reactions.[35] As discussed above in the introduction, this previously proposed model treats the plasmon excitation as similar in nature to an electron−hole pair.[20−22] However, since a surface plasmon is simply a charge density wave bound to an interface, there is no HOMO−LUMO or analogous energy separation in a plasmon excitation. Moreover, the conduction band of anatase TiO_2 is higher in energy than the Fermi energy of Au, making the direct transfer of electrons from Au to TiO_2 energetically unfavorable.

We can understand the photocatalytic enhancement observed under visible illumination by simulating the electromagnetic response of the Au nanoparticle/TiO_2 composite film using the finite-difference time-domain (FDTD) method.[36−38] Figure 6a shows a scanning electron microscope (SEM) image of the gold

dx.doi.org/10.1021/nl104005n |*Nano Lett.* 2011, 11, 1111–1116

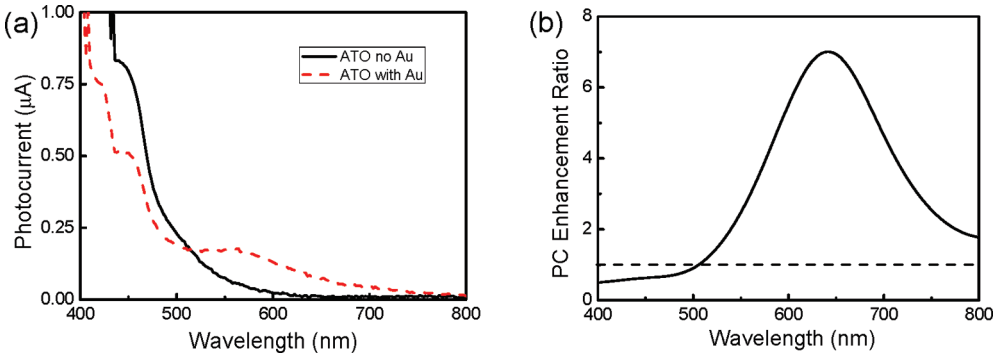

Figure 5. (a) Photocurrent spectra of anodic TiO_2 with and without Au nanoparticles. (b) Photocurrent enhancement ratio spectrum.

nanoparticle-island film deposited on top of anodic TiO_2. The light gray regions in this SEM image reflect the gold nanoparticles and the dark regions are the underlying substrate alone (or the interstitial space in between). Figure 6b−d show the simulated electromagnetic response of these Au nanoparticle/TiO_2 composites. Here, the gold regions are outlined in white in Figure 6b,c, based on the Au nanoparticle geometries from the SEM image in Figure 6a. That is, there is a one-to-one correspondence between the shapes traced out by the white lines in Figure 6b and the light gray regions in Figure 6a. The electromagnetic response of this film, as shown in Figure 6b−d, is dominated by local "hot spots" that can be seen between nearly touching Au nanoparticles. This is a well-known phenomenon in plasmonics that has been demonstrated by several research groups.[39−41] The importance of the intense local fields can be seen in Figure 6d, which shows a cross-sectional plot of the electric field distribution of one of these hot spot regions in the *z*-dimension. In this local hot spot region, the electric field intensity at the TiO_2 surface reaches 1000 times that of the incident electric field intensity. This means that the photon absorption rate (and hence electron−hole pair generation rate) is 1000 times higher than that of the incident electromagnetic radiation. This is particularly advantageous considering the small crystal grain sizes and high impurity concentrations in the anodic TiO_2,[34] which limits the minority carrier diffusion length to ∼10 nm.[42−44] As a result of this, only photons absorbed within 10 nm of the TiO_2 surface will contribute to the photocatalytic splitting of water. Here, the plasmonic nanoparticles couple light very effectively from the far-field to the near-field at the TiO_2 surface. Consequently, most of the photogenerated charge created by the plasmon excitation will contribute to the surface catalysis (water splitting).

We can calculate the photocatalytic enhancement factor based on the results of this FDTD simulation. Since the photon absorption rate (and hence electron−hole pair generation rate) is proportional to the electric field squared ($|E|^2$), we integrate $|E|^2$ over the whole film and divide by the integral of the incident electromagnetic field squared ($|E_o|^2$), as follows

$$\mathrm{EF} = \frac{\int_{-10\ \mathrm{nm}}^{0} dz \int \mathrm{d}x\,\mathrm{d}y \left|E\right|^2}{\int_{-10\ \mathrm{nm}}^{0} dz \int \mathrm{d}x\,\mathrm{d}y \left|E_o\right|^2}$$

In the *z*-dimension, we only integrate from the TiO_2 surface ($z = 0$) to one minority carrier diffusion length below the surface ($z = -10$ nm). The value for the *EF* when integrating over the whole simulation area (400 nm × 300 nm) is 12×, which is close to the values observed experimentally. This EF value was obtained for this random distribution of gold islands, not optimized geometrically. Integrating only over the area of this hot spot, as shown in Figure 6c, yields an EF of 190×. This implies that enhancement factors many times larger than this could be achieved if the geometry of this plasmonic film is optimized.[45]

Considering the fact that these hot spot regions comprise a very small fraction of the total catalytic surface area, it is remarkable that we still observe a net improvement in the photocatalytic water splitting with the addition of the gold nanoparticle film. The reason for this remarkably robust enhancement lies in the short minority carrier diffusion lengths of these anodic TiO_2 films.[46,47] The near-field optical enhancement provided by the Au nanoparticles is well matched to this defect-rich material, which has very short carrier diffusion lengths that would otherwise spoil its photocatalytic performance.[46,47] And, as stated above, virtually all of the photogenerated charge excited by these plasmon-enhanced fields contributes to the photocatalytic reaction. Doping and defects enable light absorption below the bandgap of semiconducting materials; however, this also shortens their carrier diffusion lengths and thus ultimately spoils their photocatalytic performance. Hence, there is a trade-off with doping for visible light photocatalysis. The plasmonic enhancement mechanism described here provides a way around this by coupling light to the near-field within the minority carrier diffusion length, thus making the photocatalyst more robust to defects and doping.

Several control experiments were carried out to further establish that the enhanced catalytic charge is induced electromagnetically rather than transferred directly between the plasmonic and catalytic materials. First, we tested the photocatalytic activity of the undoped TiO_2 prepared by the sol−gel method, shown in the UV−vis spectra of Figure 4. No photocurrent was observed for this material in the visible wavelength range with or without Au nanoparticles, indicating the important role of defects in the photocatalytic enhancement process under visible illumination. This substantiates our proposed mechanism of catalytic enhancement, since the previously proposed direct charge transfer model should not depend on doping. As another control experiment, we characterized nonphotocatalytic materials (e.g., ITO, glass, and quartz) covered with plasmonic Au nanoparticles. None of these samples with catalytically inactive supports showed any observable photocurrent. In the previously proposed charge transfer mechanism, the photocatalytic charge transfer with the ions in solution takes place on the Au surface, and the only relevant parameter of the TiO_2 is its conduction band

dx.doi.org/10.1021/nl104005n |*Nano Lett.* 2011, 11, 1111–1116

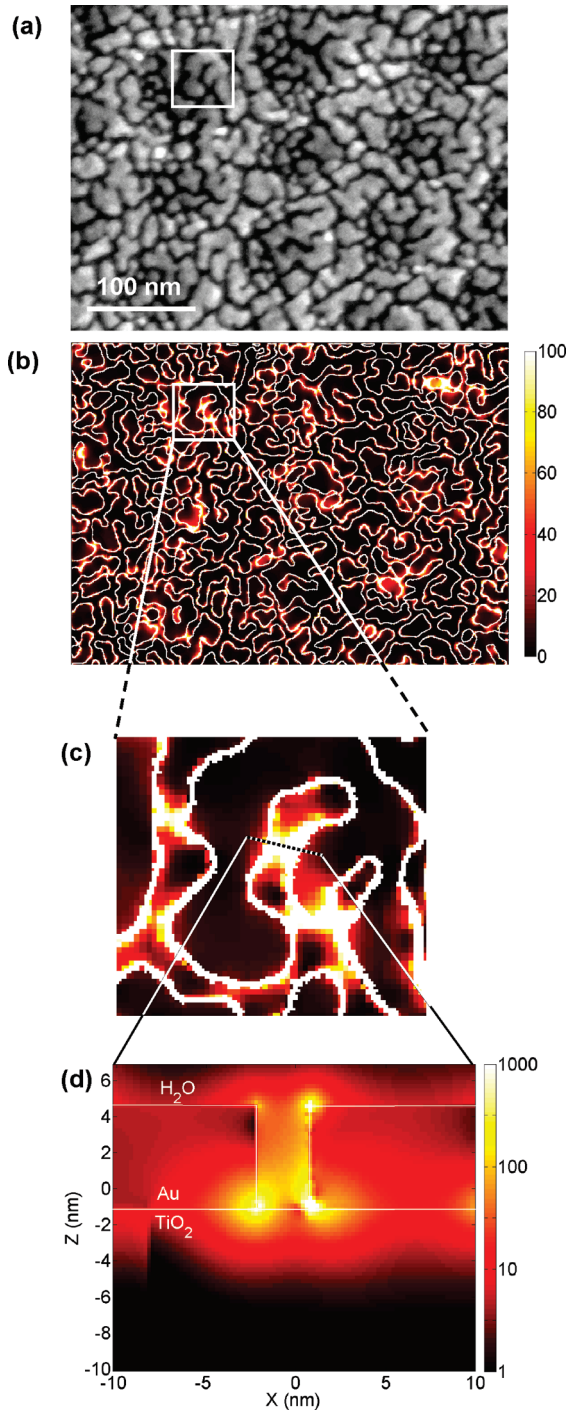

Figure 6. (a) SEM image of a 5 nm thick Au island film deposited on anodic TiO_2. (b−d) Electric field intensity at the interface of Au−TiO_2 calculated using FDTD.

energy. Since the position of the conduction band in ITO is similar to that of TiO_2, this result contradicts the previously proposed charge transfer enhancement mechanism.

Summary. In conclusion, we demonstrate enhancement in the photocatalytic splitting of water in the visible region of the electromagnetic spectrum by exploiting the surface plasmon resonance of gold nanoparticles. The intense local fields produced by the surface plasmons couple light efficiently to the surface of the TiO_2. This enhancement mechanism is particularly effective because of anodic TiO_2's short minority carrier diffusion length, which would otherwise limit its photocatalytic activity. Enhancements in the photocatalytic activity of 5× and 66× are observed at wavelengths of 532 nm and 633 nm, respectively. Electromagnetic simulations of this process suggest that enhancement factors many times larger than this are possible if this mechanism can be optimized. The experimental data and fundamental understanding described here provide a path toward resolving the photon absorption/electron diffusion length mismatch that has made photovoltaics and direct photocatalysts far too expensive to find broad applicability in our energy infrastructure. For photocatalysis, this area is especially exciting because it presents a possible route to direct solar to fuels production.

■ ASSOCIATED CONTENT

Supporting Information. ATO preparation, measurement of photocatalytic activity, and additional figures and references. This material is available free of charge via the Internet at http://pubs.acs.org.

■ ACKNOWLEDGMENT

This research was supported in part by AFOSR Award No. FA9550-08-1-0019, ARO Award No. W911NF-09-1-0240, and NSF Award No. CBET-0846725. W.H. was supported as part of the Center for Energy Nanoscience, an Energy Frontier Research Center funded by the U.S. Department of Energy, Office of Science, Office of Basic Energy Sciences under Award Number DE-SC0001013.

■ REFERENCES

(1) Fujishima, A; Honda, K. Electrochemical Photolysis of Water at a Semiconductor Electrode. *Nature* **1972**, *238*, 37.

(2) Sajjad, A. K. L.; Shamaila, S.; Tian, B. Z.; Chen, F.; Zhang, J. L. Comparative studies of operational parameters of degradation of azo dyes in visible light by highly efficient WO_x/TiO_2 photocatalyst. *J. Hazard. Mater.* **2010**, *177*, 781–791.

(3) Wang, X. H.; Li, J. G.; Kamiyama, H.; Moriyoshi, Y.; Ishigaki, T. Wavelength-Sensitive Photocatalytic Degradation of Methyl Orange in Aqueous Suspension over Iron(III)-doped TiO_2 Nanopowders under UV and Visible Light Irradiation. *J. Phys. Chem. B* **2006**, *110*, 6804.

(4) Takeuchi, M.; Yamashita, H.; Matsuoka, M.; Anpo, M.; Hirao, T.; Itoh, N.; Iwamoto, N. Photocatalytic decomposition of NO under visible light irradiation on the Cr-ion-implanted TiO_2 thin film photocatalyst. *Catal. Lett.* **2000**, *67*, 135–137.

(5) Xie, Y.; Zhao, X. J. The effects of synthesis temperature on the structure and visible-light-induced catalytic activity of F-N-codoped and S-N-codoped titania. *J. Mol. Catal. A: Chem.* **2008**, *285*, 142–149.

(6) Renger, J.; Quidant, R.; van Hulst, N.; Novotny, L. Surface-Enhanced Nonlinear Four-Wave Mixing. *Phys. Rev. Lett.* **2010**, *104*, No. 046803.

(7) Maier, S. A.; Brongersma, M. L.; Kik, P. G.; Meltzer, S.; Requicha, A. A. G.; Koel, B. E.; Atwater, H. A. Plasmonics - A route to nanoscale optical devices. *Adv. Mater.* **2001**, *13*, 1501.

(8) Kneipp, K.; Wang, Y.; Kneipp, H.; Perelman, L. T.; Itzkan, I.; Dasari, R. R.; Feld, M. S. Single Molecule Detection Using Surface-Enhanced Raman Scattering (SERS). *Phys. Rev. Lett.* **1997**, *78*, 1667–1670.

(9) Kumar, R.; Zhou, H.; Cronin, S. B. Surface-enhanced Raman spectroscopy and correlated scanning electron microscopy of individual carbon nanotubes. *Appl. Phys. Lett.* **2007**, *91*, No. 223105.

(10) Duyne, R. P. V.; Hulteen, J. C.; Treichel, D. A. Atomic force microscopy and surface-enhanced Raman spectroscopy. I. Ag island

films and Ag film over polymer nanosphere surfaces supported on glass. *J. Chem. Phys.* **1993**, *99*, 2101–2115.

(11) Jeanmaire, D.; Van Duyne, R. Surface Raman spectroelectrochemistry. Part I. Heterocyclic, aromatic, and aliphatic amines adsorbed on the anodized silver electrode. *J. Electroanal. Chem.* **1977**, *84*, 1–20.

(12) Boyd, D. A.; Greengard, L.; Brongersma, M.; El-Naggar, M. Y.; Goodwin, D. G. Plasmon-Assisted Chemical Vapor Deposition. *Nano Lett.* **2006**, *6*, 2592–2597.

(13) Hung, W. H.; Hsu, I. K.; Bushmaker, A.; Kumar, R.; Theiss, J.; Cronin, S. B. Laser Directed Growth of Carbon-Based Nanostructures by Plasmon Resonant Chemical Vapor Deposition. *Nano Lett* **2008**, *8*, 3278–3282.

(14) Endo, T.; Kerman, K.; Nagatani, N.; Hiepa, H. M.; Kim, D. K.; Yonezawa, Y.; Nakano, K.; Tamiya, E. Multiple Label-Free Detection of Antigen-Antibody Reaction Using Localized Surface Plasmon Resonance-Based Core−Shell Structured Nanoparticle Layer Nanochip. *Anal. Chem.* **2006**, *78*, 6465–6475.

(15) Sha, M. Y.; Xu, H.; Penn, S. G.; Cromer, R. SERS nanoparticles: a new optical detection modality for cancer diagnosis. *Nanomedicine* **2007**, *2*, 725–34.

(16) Awazu, K.; Fujimaki, M.; Rockstuhl, C.; Tominaga, J.; Murakami, H.; Ohki, Y.; Yoshida, N.; Watanabe, T. A Plasmonic Photocatalyst Consisting of Silver Nanoparticles Embedded in Titanium Dioxide. *J. Am. Chem. Soc.* **2008**, *130*, 1676–1680.

(17) Christopher, P.; Ingram, D. B.; Linic, S. Enhancing photochemical activity of semiconductor nanoparticles with optically active Ag nanostructures: photochemistry mediated by Ag surface plasmons. *J. Phys. Chem. C* **2010**, *114*, 9173–9177.

(18) Hung, W. H.; Aykol, M.; Valley, D.; Hou, W. B.; Cronin, S. B. Plasmon Resonant Enhancement of Carbon Monoxide Catalysis. *Nano Lett.* **2010**, *10*, 1314–1318.

(19) Nakayama, K.; Tanabe, K.; Atwater, H. A. Plasmonic nanoparticle enhanced light absorption in GaAs solar cells. *Appl. Phys. Lett.* **2008**, *93*, No. 121904.

(20) Tian, Y.; Tatsuma, T. Plasmon-induced photoelectrochemistry at metal nanoparticles supported on nanoporous TiO_2. *Chem. Commun.* **2004**, 1810–1811.

(21) Kowalska, E.; Mahaney, O. O. P.; Abe, R.; Ohtani, B. Visible-light-induced photocatalysis through surface plasmon excitation of gold on titania surfaces. *Phys. Chem. Chem. Phys.* **2010**, *12*, 2344–2355.

(22) Tian, Y.; Tatsuma, T. Mechanisms and applications of plasmon-induced charge separation at TiO_2 films loaded with gold nanoparticles. *J. Am. Chem. Soc.* **2005**, *127*, 7632–7637.

(23) O'Regan, B.; Graetzel, M. A low-cost, high-efficiency solar cell based on dye-sensitized colloidal TiO_2 films. *Nature* **1991**, *353*, 737.

(24) Gratzel, M. Photoelectrochemical cells. *Nature* **2001**, *414*, 338–344.

(25) Grimes, C. A. Synthesis and application of highly ordered arrays of TiO_2 nanotubes. *J. Mater. Chem.* **2007**, *17*, 1451–1457.

(26) Nakabayashi, S.; Kira, A. Surface-Trapped Charge at CDS Electrode in Aqueous-Solution As Observed by Photoreflectance Spectroscopy. *J. Phys. Chem.* **1991**, *95*, 9961–9965.

(27) Serpone, N.; Lawless, D.; Khairutdinov, R. Size Effects on the Photophysical Properties of Colloidal Anatase TiO_2 Particles-Size Quantization or Direct Transitions in This Indirect Semiconductor. *J. Phys. Chem.* **1995**, *99*, 16646–16654.

(28) Bendavid, A.; Martin, P. J.; Jamting, A.; Takikawa, H. Structural and optical properties of titanium oxide thin films deposited by filtered arc deposition. *Thin Solid Films* **1999**, *355*, 6–11.

(29) Li, Q.; Shang, J. K. Self-Organized Nitrogen and Fluorine Co-doped Titanium Oxide Nanotube Arrays with Enhanced Visible Light Photocatalytic Performance. *Environ. Sci. Technol.* **2009**, *43*, 8923–8929.

(30) Hryciw, A. C.; Jun, Y. C.; Brongersma, M. L. Plasmon-enhanced emission from optically-doped MOS light sources. *Opt. Express* **2009**, *17*, 185–192.

(31) Liu, Z.; Hung, W. H.; Aykol, M.; Valley, D.; Cronin, S. B. Optical manipulation of plasmonic nanoparticles, bubble formation and patterning of SERS aggregates. *Nanotechnology* **2010**, *21*, 105304.

(32) Adleman, J. R.; Boyd, D. A.; Goodwin, D. G.; Psaltis, D. Heterogenous Catalysis Mediated by Plasmon Heating. *Nano Lett.* **2009**, *9*, 4417–4423.

(33) Yen, C.-W.; El-Sayed, M. A. Plasmonic Field Effect on the Hexacyanoferrate (III)-Thiosulfate Electron Transfer Catalytic Reaction on Gold Nanoparticles: Electromagnetic or Thermal? *J. Phys. Chem. C* **2009**, *113*, 19585–19590.

(34) Varghese, O. K.; Gong, D.; Paulose, M.; Grimes, C. A.; Dickey, E. C. Crystallization and high-temperature structural stability of titanium oxide nanotube arrays. *J. Mater. Res.* **2003**, *18*, 156–165.

(35) Tian, Y.; Tatsuma, T. Mechanisms and Applications of Plasmon-Induced Charge Separation at TiO_2 Films Loaded with Gold Nanoparticles. *J. Am. Chem. Soc.* **2005**, *127*, 7632–7637.

(36) Taflove, A.; Hagness, S. C. *Computational electrodynamics: the finite-difference time-domain method*, 3rd ed.; Artech House: Boston, MA, 2005; pp xxii, 1006.

(37) Le, F.; Brandl, D. W.; Urzhumov, Y. A.; Wang, H.; Kundu, J.; Halas, N. J.; Aizpurua, J.; Nordlander, P. Metallic Nanoparticle Arrays: A Common Substrate for Both Surface-Enhanced Raman Scattering and Surface-Enhanced Infrared Absorption. *ACS Nano* **2008**, *2*, 707–718.

(38) Zou, S. L.; Schatz, G. C. Silver nanoparticle array structures that produce giant enhancements in electromagnetic fields. *Chem. Phys. Lett.* **2005**, *403*, 62–67.

(39) Hao, E.; Schatz, G. C. Electromagnetic fields around silver nanoparticles and dimers. *J. Chem. Phys.* **2003**, *120*, 357.

(40) Oubre, C.; Nordlander, P. Finite-Difference Time-Domain Studies of the Optical Properties of Nanoshell Dimers. *J. Phys. Chem. B* **2005**, *109*, 10042.

(41) Jiang, J.; Bosnick, K.; Maillard, M.; Brus, L. Single Molecule Raman Spectroscopy at the Junctions of Large Ag Nanocrystals. *J. Phys. Chem. B* **2003**, *107*, 9964.

(42) Leng, W. H.; Barnes, P. R. F.; Juozapavicius, M.; O'Regan, B. C.; Durrant, J. R. Electron Diffusion Length in Mesoporous Nanocrystalline TiO_2 Photoelectrodes during Water Oxidation. *J. Phys. Chem. Lett.* **2010**, *1*, 967–972.

(43) Savenije, T. J.; Warman, J. M.; Goossens, A. Visible light sensitization of titanium dioxide using a phenylene vinylene polymer. *Chem. Phys. Lett.* **1998**, *287*, 148–153.

(44) Arango, A. C.; Johnson, L. R.; Bliznyuk, V. N.; Schlesinger, Z.; Carter, S. A.; Horhold, H. H. Efficient titanium oxide/conjugated polymer photovoltaics for solar energy conversion. *Adv. Mater.* **2000**, *12*, 1689.

(45) Pavaskar, P.; Cronin, S. B. Iterative optimization of plasmon resonant nanostructures. *Appl. Phys. Lett.* **2009**, *94*, 760818–760818−10.

(46) Liu, K. S.; Fu, H. G.; Shi, K. Y.; Xiao, F. S.; Jing, L. Q.; Xin, B. F. Preparation of Large-Pore Mesoporous Nanocrystalline TiO_2 Thin Films with Tailored Pore Diameters. *J. Phys. Chem. B* **2005**, *109*, 18719–18722.

(47) Smarsly, B.; Grosso, D.; Brezesinski, T.; Pinna, N.; Boissiere, C.; Antonietti, M.; Sanchez, C. Highly Crystalline Cubic Mesoporous TiO_2 with 10 nm Pore Diameter Made with a New Block Copolymer Template. *Chem. Mater.* **2004**, *16*, 2948–2952.